
Generating compressor maps to simulate starting and windmilling

Joachim Kurzke
kurzke@gasturb.de
Max Feldbauer Weg 5
85221 Dachau
Germany

ABSTRACT

Physically sound compressor maps are the key to accurate aircraft engine performance simulations. Usually, calculated and measured maps only cover the speed range between idle and full thrust. Simulation of starting, windmilling and re-light requires maps which include sub-idle speed values as well as the region in which the pressure ratio is less than unity.

Engineers outside industry, at universities and research facilities, usually do not have access to the special rigs needed for measuring locked rotor (zero-speed line) characteristics, nor do they have the geometric data needed for CFD calculations. In the following paper, a new map extension method is described which employs interpolation with a zero-speed line zero that needs neither data from an experiment with a locked rotor nor compressor geometry information. Zero speed torque and pressure losses are derived from correlations embedded in the map to be extended.

Incompressible flow theory applies in a significant part of the compressor map. In this region a linear relationship exists between torque/flow and flow. The slope of this relationship is independent of speed and can be found from the speed lines for which data are available.

Compressibility effects correlate with the Mach number level in the exit guide vane (EGV). Some simple considerations lead to a model that is applicable generally for the flow conditions in the EGV at any point in the map.

The underlying theory is explained and compared with data from three different compressors. Besides adding the sub-idle map region, the map is also extended to low pressure ratio at high speeds. The approach is then applied to the map of a single stage transonic fan designed for a high bypass engine.

Keywords: Gas Turbine Performance; Compressor Map Generation; Starting and Windmilling

NOMENCLATURE

EGV Exit Guide Vane

Symbols

blk	blockage
c_1, c_2, \dots	constant values
F	force
H	specific work
i	incidence
M	Mach number
N	relative rotational speed
P	total pressure
T	total temperature
Trq	torque
U	circumferential speed
V_{ax}	axial velocity
W	(corrected) mass flow
$W_{R,ex}$	corrected exit mass flow
α_1	stator exit flow angle
β_2	rotor blade exit flow angle
β	map coordinate
Φ	flow coefficient V_{ax}/U
Ψ	work coefficient H/U^2
Π	pressure ratio
ω	rotational speed

1.0 INTRODUCTION

In recent years, several papers addressing sub-idle and windmilling performance of compressors have been published. The first reference (Ferrer-Vidal et al., 2018) gives an extensive overview of various approaches to the problem. The compressor sub-idle map generation method presented uses interpolation between the zero-speed line (i.e. locked rotor torque and pressure loss) and idle speed. The windmilling characteristic (zero specific work, pressure ratio less than 1) is regarded as an important addition to the interpolation process. The data for locked rotor and windmilling performance are either measured in a special rig or generated from a CFD calculation. So, the application of the method relies on information which is extremely rare.

A very detailed examination of similarity principles and scaling laws for windmilling fans is given in Prasad 2018. One of the conclusions there is, that radial distribution of the flow need not be considered - it is enough to work with average values. Prediction of the windmilling speed of a single stage fan requires knowledge of three loss coefficients, which are the result of a single numerical simulation at any one windmilling condition. The detailed rotor and vane geometry must be known for the application of the method, a prerequisite which is rarely fulfilled.

Another comprehensive literature overview (Ferrand et. al., 2018) comments on various methods for compressor map extrapolation to sub-idle speed. Windmilling is not considered because it did not feature in that specific study.

Extending an existing map by extrapolation usually uses similarity laws for incompressible flow and starts with the data from the last known speed. The quality of the extrapolation can be improved by taking compressibility effects into consideration (Gaudet, 2007 and Zhitao Wang et al., 2015). An experimental validation of this extrapolation method is found in (Hönle et al., 2013).

Other extrapolation methods are based on the two lowest speed lines with data from either measurements or calculations. These speed lines can contain compressibility effects which need special treatment, otherwise peculiar results show up in the high flow coefficient region of the extrapolated lines.

2.0 THEORY

2.1 Work and flow coefficient

If we consider the form of the ψ - Φ relationship for a single stage compressor with symmetrical velocity triangles in simple terms, we can conclude that ψ is a linear function of Φ . This follows from the fact that the flow leaves a blade or vane row in the direction given by the trailing edge geometry.

$$\psi = 1 - \Phi * (\tan \alpha_1 + \tan \beta_2) = 1 - c_1 * \Phi \quad (1)$$

Work input H is a straight line when plotted as Ψ over Φ , whereas work output H_{is} calculated from pressure ratio is not (see Fig. 1). The losses in the compression process, described by efficiency $\eta = H_{is}/H$, are smallest at the peak efficiency point.

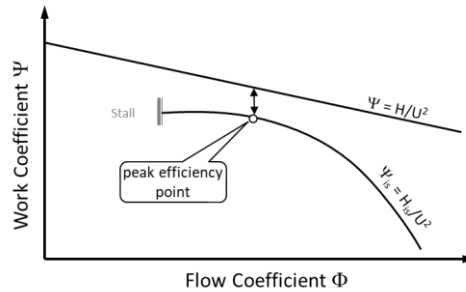


Figure 1: Peak efficiency point of the ψ - Φ correlation

The only prerequisite for the validity of equation 1 is that the flow direction downstream of the blades and vanes is enforced by the geometry of the blades and vanes. In an incompressible fluid (constant density) there is only one curve for $\psi_{is}=f(\Phi)$ and this is valid for any speed.

For a given geometry, a change in fluid density causes a change in velocity and consequently the value of the flow coefficient is affected. The function $\psi_{is}=f(\Phi)$ is no longer independent of speed. This has been recognized and has led to the recommendation of modified similarity laws whose structure is quite complex (Gaudet, 2007 and Zhitao Wang et al., 2015).

A simpler approach to the problem consists of a speed-dependent density correction factor applied to the flow coefficient. Density is calculated for each speed line and normalized by the density at a convenient reference point.

The flow correction factor is the density ratio, modified by an empirically determined exponent. From the examination of many maps (Kurzke, 2012) it was found, that a correction factor for the flow coefficient of $(\rho(N)/\rho_{ref})^{0.5}$ makes the $\psi_{is}=f(\Phi)$ relationship independent of speed, especially at low speeds and low Φ .

Figure 2 shows measured data from a single stage compressor (page 12 of the map collection, Kurzke 2012) together with lines for Ψ and Ψ_{is} plotted against density-corrected flow coefficient Φ . The Ψ lines are linear for $\Phi_{rel}<1$, even at the highest speed ($N=1$). They bend downwards progressively with increasing speed due to high Mach number effects.

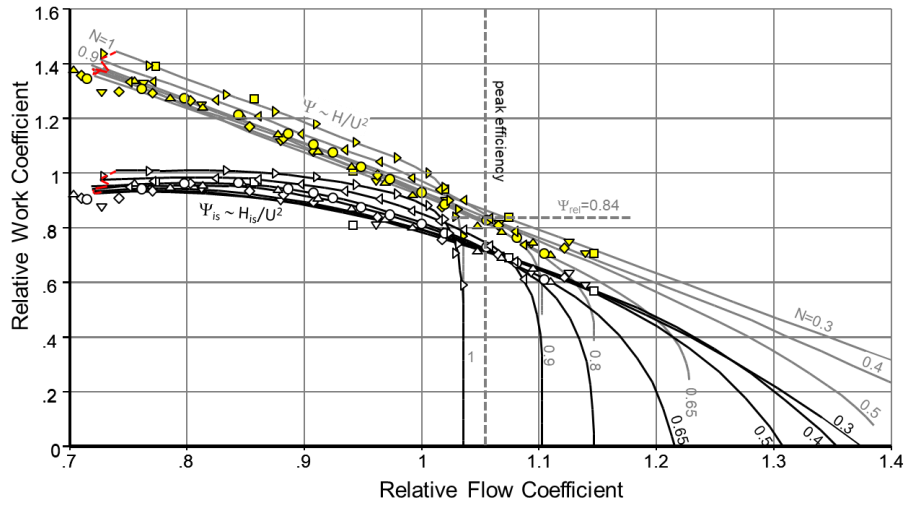


Figure 2: Ψ - Φ correlations from a single compressor stage

Figure 3 shows the efficiency values corresponding to figure 2. For all speeds below $N=0.9$, peak efficiency values occur roughly at a flow coefficient $\Phi_{rel} \approx 1.05$. Reading figure 2 at that value yields $\Psi_{rel} \approx 0.84$ for the peak efficiency point.

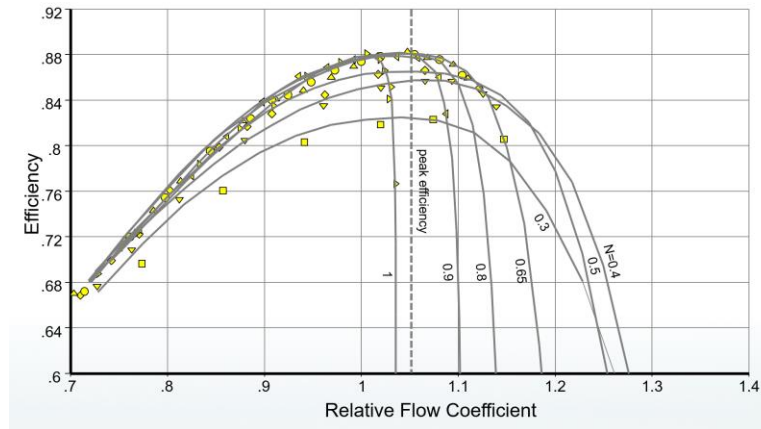


Figure 3: Efficiency corresponding with figure 2

Note that none of the measured data points are in the region $\Phi_{rel} > 1.15$. No obvious rule to extrapolate the map to much higher Φ values can be extracted from the two figures.

2.2 Torque

Compressor power can be expressed as the product of flow and specific work as well as the product of angular speed and torque:

$$PW = W * H = \omega * Trq \quad (2)$$

Rearrangement and insertion of equation 1 yields

$$\frac{Trq}{W^2} = c_2 * \frac{H}{U^2} * \frac{U}{W} = c_2 * \frac{1 - c_1 * \Phi}{\Phi} = c_2 * \frac{1}{\Phi} - c_1 * c_2 \quad (3)$$

This equation is valid where flow velocity V_{ax} is proportional to mass flow W . Under this condition, Trq/W^2 is a linear function of $1/\Phi$ and Trq/W is – for a given circumferential speed - a linear function of W :

$$\frac{Trq}{W} = c_3 * U - c_4 * W \quad (4)$$

Analysis of many maps from single and multi-stage axial compressors shows that the low mass flow part of the torque/flow=f(flow) correlation for constant speed is linear for relative speeds below a certain value.

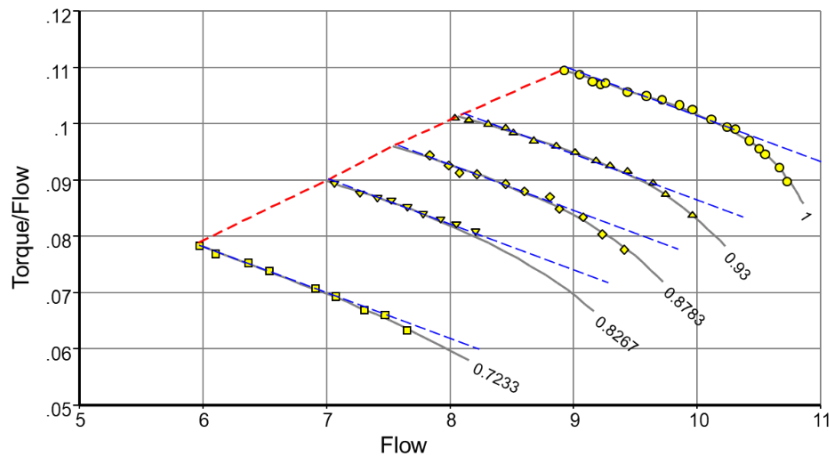


Figure 4: Torque/flow lines in a map from a three-stage compressor (data from Lippett et al., 2005)

Figure 4 shows that equation 4 is in line with measured data in the low mass flow parts of the speed lines. Note that the dashed lines are exactly parallel. This is remarkable because the data are from a three-stage compressor while equation 4 has been derived for a single stage machine.

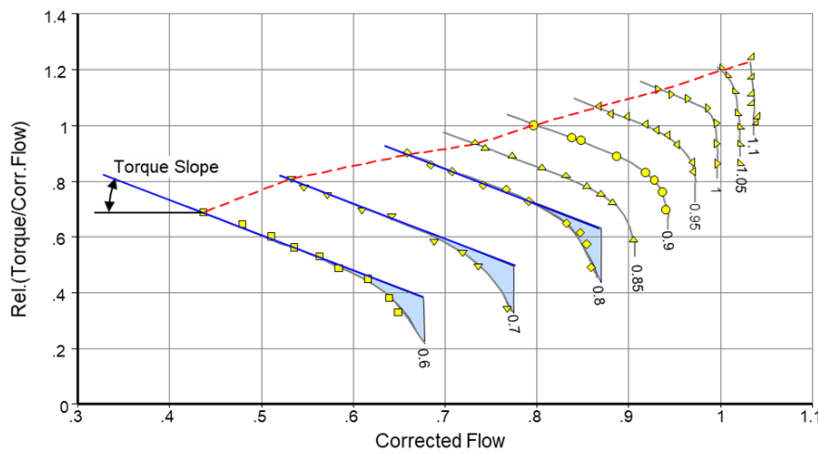


Figure 5: Torque/flow lines in the map of a single stage transonic fan (data from Cumpsty, 2015)

The lines bend downwards at higher mass flows with a lower Mach number level at the compressor design point giving longer straight parts for the torque/flow =f(flow) lines.

2.3 The zero-speed line

The zero-speed line has some special properties which cannot be described with a ψ - Φ correlation. With a locked rotor, the compressor may be considered as a pipe with restrictions. Total temperature is constant because no work is transferred. Total pressure decreases from the inlet to the exit of the compressor. For incompressible flow, the zero-speed line – i.e. the pressure ratio=f(flow) correlation - is a parabola.

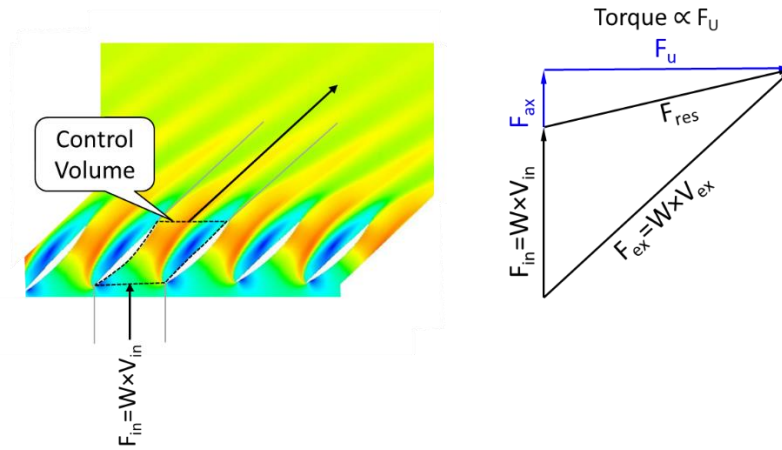


Figure 6: Forces on a locked rotor
(CFD background picture from Aslanidou, 2010)

The locked rotor changes the direction of the fluid and downstream of the blades this is determined by the blade exit geometry. The momentum at the control volume inlet corresponds to the force vector $F_{in} = W \times V_{in}$, which has no circumferential component. At the control volume exit, however, there is a force in the circumferential direction, and this is proportional to the torque exerted by the fluid on the locked rotor.

Since inlet velocity is proportional to mass flow, specific torque Trq/W is proportional to flow W . Thus equation 4 is also valid for the locked rotor!

2.4 Exit guide vane

At low speed, when almost no increase in density occurs, the maximum mass flow is restricted by the smallest area in the flow path. This is the throat area of the exit guide vane (EGV) which is sized for the high fluid density at the compressor design point. An extreme case is the locked rotor, because then the density at the entrance to the EGV is lower than that at the compressor inlet and therefore the Mach number in the EGV throat is higher than that at the compressor inlet.

A representative value for the throat area of the EGV can be derived from an assumed throat Mach number at a map reference point (the compressor design point). Mach number sets the corrected flow per area; total pressure at the entrance to the EGV (which is slightly higher than the compressor delivery pressure) as well as the compressor delivery total temperature are easily calculated.

When the EGV throat Mach number at one point in the map is known, it can be derived at any other point in the map from the compressor exit conditions and the EGV throat area.

The total pressure loss of the EGV is proportional to the square of corrected flow at the compressor exit if the flow direction is approximately equal to the EGV design inlet angle. High incidence leads to flow separation, increased losses and blockage of the flow area (Prasad, 2018).

Precise calculation of EGV total pressure loss and blockage would require knowledge of the detailed geometry as well as the flow direction downstream of the last rotor. However, an approximation of the conditions at the EGV throat can be found from the following considerations.

The flow leaves the compressor in the axial direction. A single row of exit guide vanes changes the flow direction typically by 30° at the design point, where incidence is assumed to be zero. If the flow direction downstream of the last rotor is 45° , then the EGV design point inlet velocity triangle looks reasonable.

Let us postulate that the flow direction downstream of the last rotor remains at 45° at off-design. This is equivalent to the hypothesis which led to equations 1 and 4 and allows the EGV incidence and total pressure loss to be calculated for any point in the map.

In this model the throat area blockage is due to flow separation only, which is a function of incidence. Negative incidence up to -15° does not cause any blockage, but beyond that it increases progressively. This generic model creates blockage factors for windmilling of the order of 30 to 40%, which is in line with literature (Prasad 2018 and Zachos 2011).

Staying with this approach requires a guess for the location of the compressor design point in the map. The EGV throat Mach number at this point is an input quantity. There are two criteria for checking if the reference Mach number is a reasonable choice.

In figure 7, the EGV throat Mach number is at a reasonable level for all measured data points. The assumption of a significantly higher reference point Mach number would move all the points upwards and some would be on the Mach=1 line. Moreover, there would be a range of corrected flow values at sonic flow and this cannot be, since it would contravene the laws of physics.

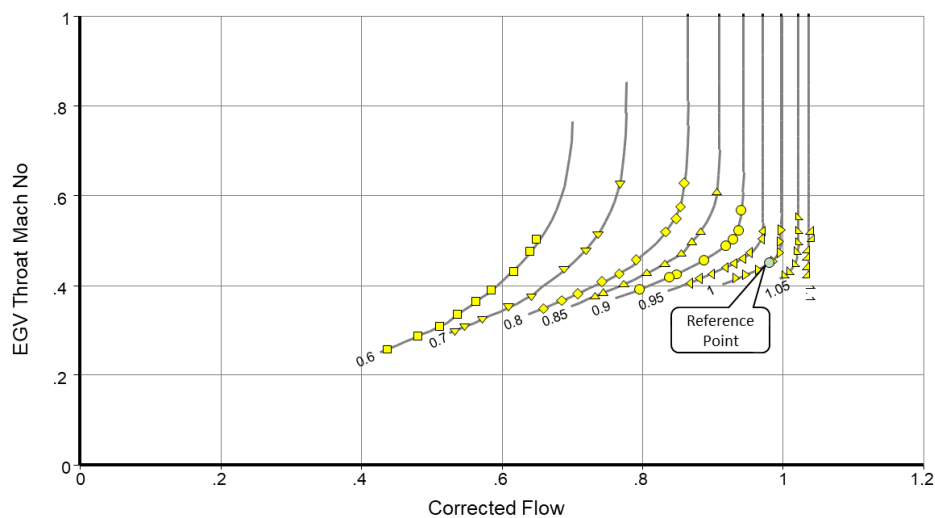


Figure 7: A reasonable choice for EGV Mach number at the reference point

The second criterion for the reference point EGV throat Mach number is illustrated in figure 8. There a boundary for the map region is shown where incompressible flow theory is applicable. Above the limit line the torque/flow lines are straight and bend downwards below and to the right of the incompressible flow boundary.

The two criteria are not stringent, they are somewhat soft. Nevertheless, for an experienced engineer, choosing a representative EGV throat Mach number at the map reference point should be possible.

2.5 Compressibility effects

Mean density changes with speed and affects flow coefficient values, as discussed in section 2.1. This phenomenon is different from the compressibility effects that bend the speed lines downwards relative to the shape postulated by incompressible theory, which are caused by high Mach numbers within the compressor flow field in general. The degree of speed lines turning correlates with the EGV throat Mach number and speed that can be seen in figure 9 and which is consistent with figure 8.

Figure 9 is very well suited for extrapolating the map towards lower speed.

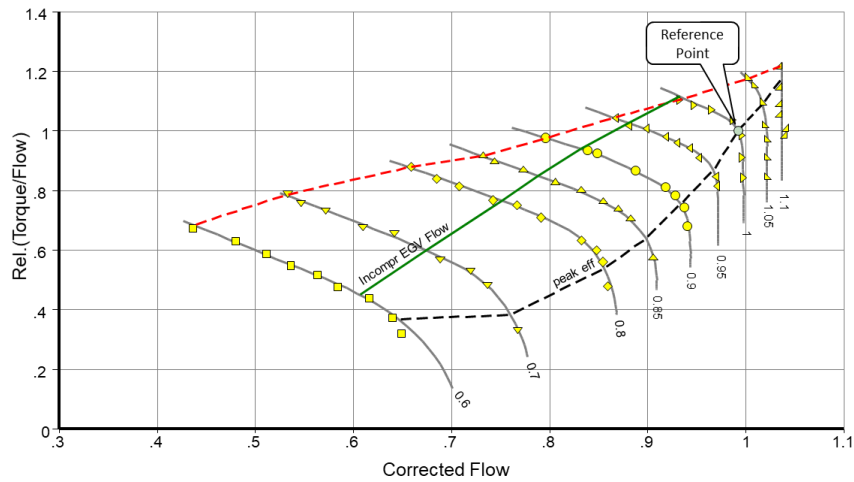


Figure 8: Limit for incompressible flow (EGV throat Mach number = 0.4)

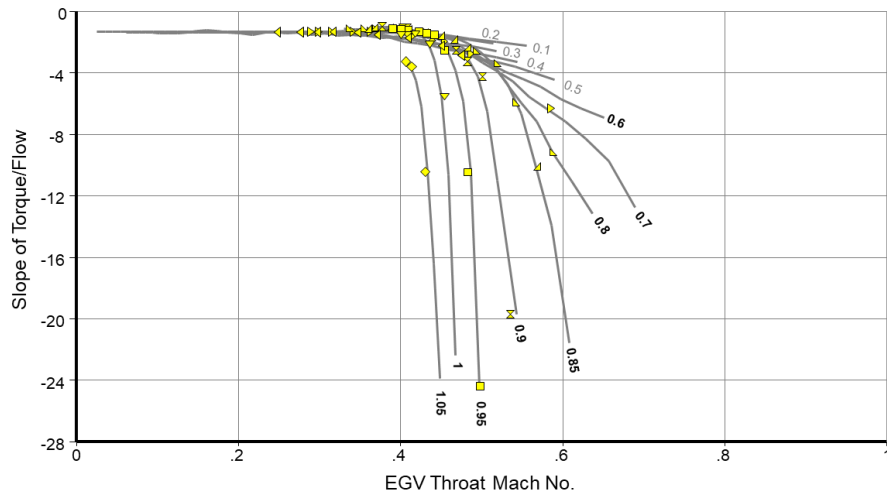


Figure 9: Compressibility effects found in the map of a transonic fan

Another quantity which correlates with EGV throat Mach number is specific work and figure 10 is especially useful for extending a map in the high speed – low pressure ratio region. Decreasing pressure ratio at high speed corresponds to increasing the EGV throat Mach number until it chokes. Further reduction of pressure ratio will not affect specific work because this is done only in the rotor(s). It is reasonable to assume that the approach to sonic conditions in the EGV is smooth and the curve $H=f(M_{EGV})$ is horizontal when it reaches $M_{EGV}=1$.

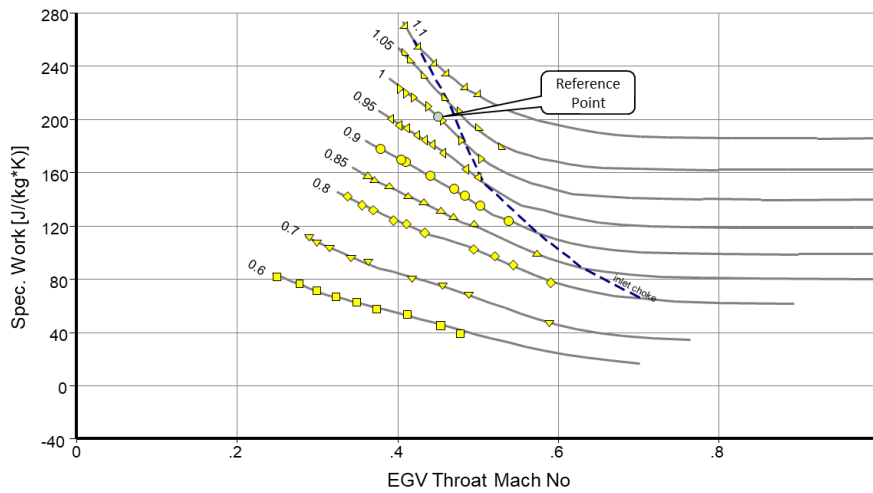


Figure 10: Specific work at high speed is limited by EGV choke

2.6 Map regions

For map extension purposes, the various parameter correlations outlined apply optimally to different regions:

- The Ψ - Φ and η - Φ relationships are most useful where efficiency is high, and speed is low.
- It is not practical to work with efficiency in the low speed region where pressure ratio is one or lower, but this problem can be addressed by using specific work or torque/flow=f(flow).
- The downward bending of speed lines due to compressibility effects in the low speed region can be quantified using the relationship between torque slope and EGV throat Mach number.
- In the region where high speed is combined with low pressure ratio, there is a lower limit for specific work caused by EGV choking.

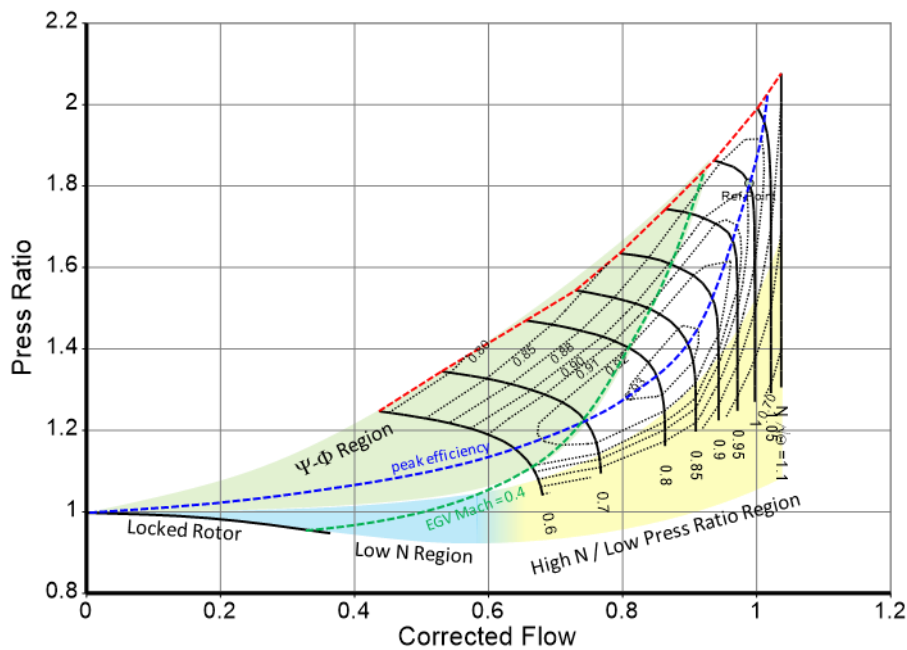


Figure 11: Map regions

3.0 APPLICATION

3.1 General

The approach is implemented in the most recent version of Smooth C, a publicly available software presented for the first time in the nineteen-nineties (Kurzke 1996). This program is a specialized plotting program which helps a performance engineer generate smooth meaningful lines through a cloud of measured or calculated data points. Many graphs show the measured data together with the lines in figures with physically meaningful parameters and allow checking whether the result makes sense or not.

3.2 Baseline map

The fan map shown previously in figures 5 and 7 - 11 (Cumpsty 2015) serves to illustrate the extrapolation. This map is from a transonic single stage compressor designed for use in a turbofan engine with medium bypass ratio.

If the design point of the fan were known, then this would be the first choice for the map. However, nothing is known about the design details, not even the absolute efficiency. The maximum efficiency point on the speed line 1.0 serves as the reference point.

3.3 Smoothing the map

First, an auxiliary coordinate system consisting of 20...30 parabolas is defined. These so-called β lines have no physical meaning generally; they are introduced for the sole purpose of reading the map unambiguously in a performance program. However, the parabolas can be selected in such a way that they approximate lines of constant work coefficient $\Psi=H/U^2$ very well.

The map table output is restricted by a lower parabola (labelled $\beta=0$) and an upper parabola (labelled $\beta=1$). The upper parabola passes through the origin (flow=0, pressure ratio = 1).

In smoothing the map, it must be ensured that torque/flow=f(flow) is a straight line in the incompressible flow region of the lowest available speed. This is important because the torque/flow line for zero speed will be parallel to the corresponding part of the lowest speed line.

3.4 Extension to low pressure ratio

During windmill reight simulations it might happen that part of the transient operating line lies in the map region where speed is high and pressure ratio is low. Frequently no measured data are available in this location, so an extrapolation is required. Figures 10, 12 and 13 are especially helpful in this task.

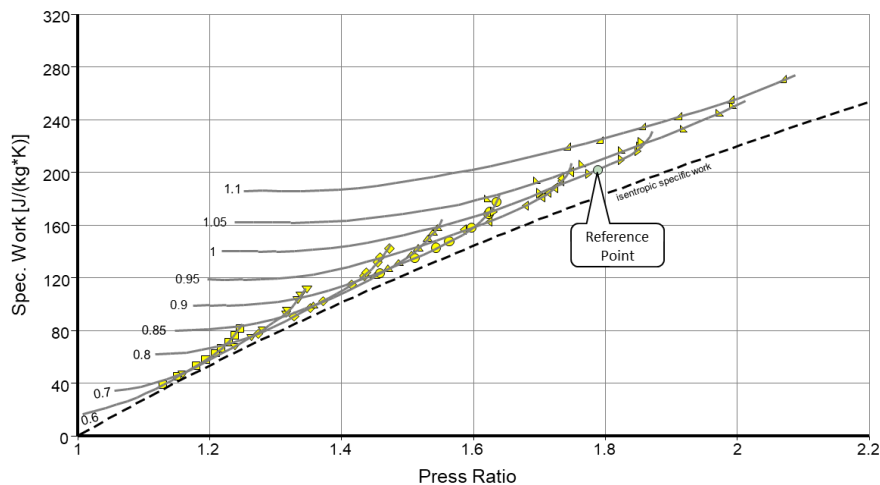


Figure 12: Specific work vs. pressure ratio

As explained earlier, choking of the exit guide vane sets a lower limit for specific work. This limit is approached in a smooth transition seen in figures 10 and 12. However, it is difficult to see from these figures precisely how the minimum specific work changes with speed. Figure 13 resolves that problem: it shows specific work for constant β against speed squared.

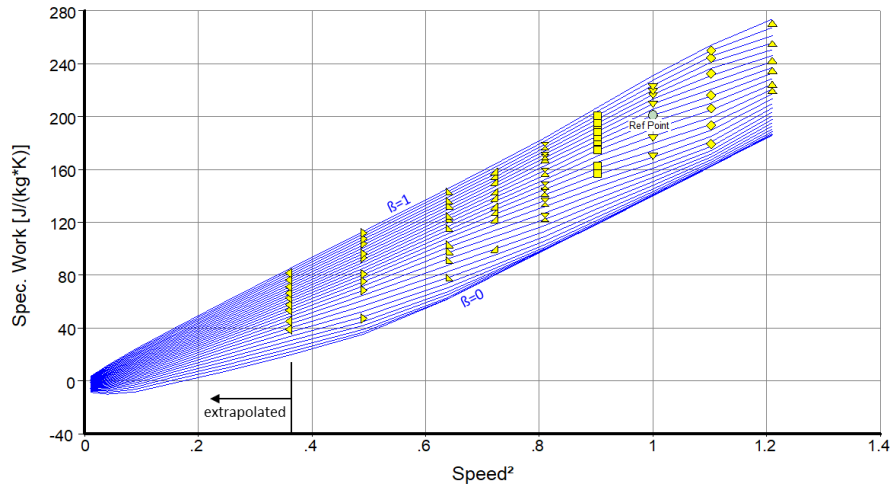


Figure 13: Specific work vs. speed squared with β -lines

Note that this map extension does not provide exact values for the format of specific work versus pressure ratio. The uncertainty of the extrapolation increases as pressure ratio falls.

3.5 Extension to low speed

The map extension procedure for sub-idle speed begins by guessing the zero-speed line. Specific work of a locked rotor is zero; the pressure ratio versus flow behaviour is parabolic; isentropic specific work follows from the pressure ratio. The slope of the torque/flow= $f(\text{flow})$ correlation is constant and equal to that in the high pressure ratio part of the last speed line verified by measured data. Both isentropic and actual specific work are zero at the point pressure ratio = unity, mass flow = zero. A pre-condition for the following procedure is that the upper β -line passes through that point.

Map extension is a stepwise process in which one speed line is interpolated after another. In our example, the first additional speed line is $N=0.5$. Isentropic specific work is found from quadratic interpolation along the β -lines between the value at zero speed and that at the lowest verified speed ($N=0.6$).

Actual specific work is interpolated similarly on the upper parabola ($\beta=1$) - it is proportional to speed squared, since specific work for the locked rotor is zero. At the $\beta=1$ point for the interpolated speed, a straight line of torque/flow= $f(\text{flow})$ commences, parallel to the equivalent locked rotor line. This procedure yields the values of specific work and efficiency at each cross point of the torque line with a β -line.

Modifying the assumption for the pressure loss characteristic of the locked rotor affects the interpolated line, especially which value of Φ the peak efficiency corresponds to. Figure 3 shows that, in the Ψ - Φ region of the map, the peak efficiency value always occurs at the same value of Φ or Ψ .

If equation 4 is re-written as

$$\frac{Trq}{W} = W * \left(c_3 * \frac{1}{\Phi} - c_4 \right) \quad (5)$$

it can be stated that torque/flow is proportional to flow for a given value of Φ . Therefore, all peak efficiency points must be on a straight line in figure 14. This condition is the means by which the locked rotor pressure loss assumption is reconciled with the known compressor map data.

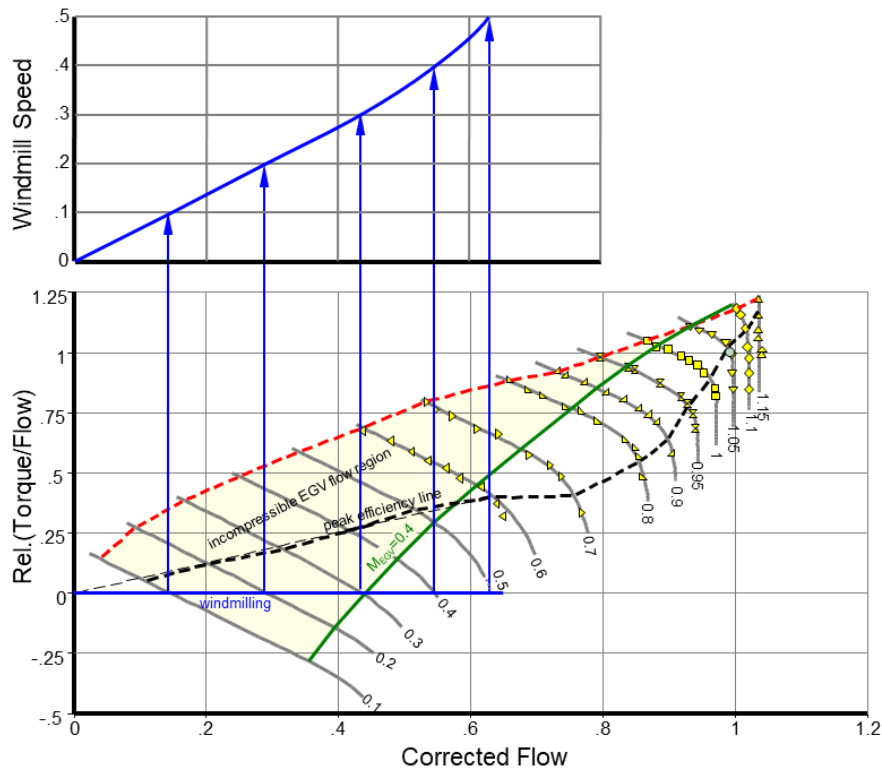


Figure 14: Peak efficiency line in the torque/flow=f(flow) diagram and windmilling speed-flow relationship

After this first working step, the torque/flow=f(flow) relationship is still linear. The second part of the speed line creation process applies the compressibility correction derived from the correlation of torque slope with EGV throat Mach number. The amount the speed lines in figure 14 bend downwards outside the incompressible EGV flow region must be consistent with figures 9 and 13.

After the interpolated speed line 0.5 has been adjusted such that its peak efficiency point is on the thin dashed straight line through the origin of figure 14, the next line can follow. The 0.4 speed line results from the interpolation between the speed line 0.5 and the locked rotor line, the speed line 0.3 is based on the line $N=0.4$ and so on. All the sub-idle speed lines in figure 14 have been found using this procedure.

Figure 15 shows the final map extension in a standard format, while figures 9, 13 and 14 contain many interesting additional details. The upper part of figure 14 shows the variation of windmilling speed with corrected flow. As expected, the low speed portion of this correlation is linear.

The picture collection of the compressor map preparation program Smooth C offers many more illustrations of relevant parameter relationships.

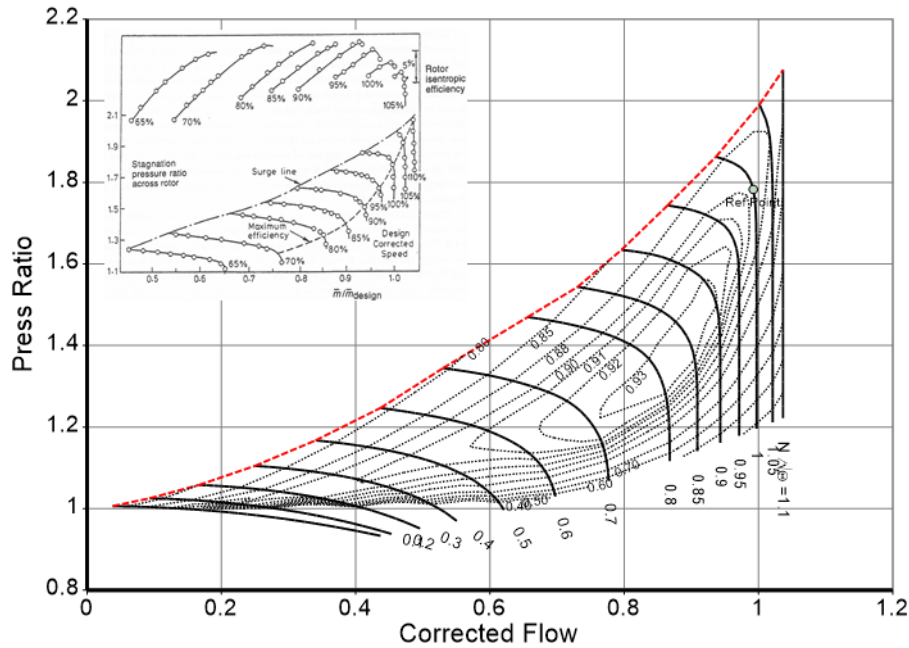


Figure 15: Extended map based on (Cumpsty, 2015)

4.0 CONCLUDING REMARKS

The accuracy of the map extension is not very sensitive to the assumption for the EGV throat Mach number at the reference point. The biggest source of error is the uncertainty of the torque/flow= $f(\text{flow})$ line slope. This should be rigorously evaluated from the measured data, considering all the relevant available data.

The EGV simulation provides a guide for the map extension. It is not an exact science but only an approximation. Only one input is required, namely the EGV throat Mach number at the reference point. Using more would complicate the method without adding significantly to the accuracy of the result.

The approach is implemented in the software Smooth C and has been successfully applied to many compressor maps from the open literature. Starting and windmill reflight simulations have been demonstrated successfully in GasTurb.

ACKNOWLEDGMENTS

Many thanks to the GasTurb team in Aachen, especially Markus Pohl who has checked the software thoroughly. Thanks also to Ian Halliwell and Robert Hill (the co-author and the editor of “Propulsion and Power”) for their valuable hints.

REFERENCES

- [1] L.E. FERRER-VIDAL, V. PACHIDIS, R.J. TUNSTALL “An enhanced compressor sub-idle map generation method”, *Global Power and Propulsion Society*, GPPS-2018-0004, 2018
- [2] D. PRASAD, “Aerodynamic similarity principles and scaling laws for windmilling fans”, *ASME GT2018-76640*, 2018
- [3] A. FERRAND, M. BELLENOUE, Y. BERTIN, R. CIRLIGEANU, P. MARCONI, F. MERCIER-CALVAIRAC “High fidelity modelling of the acceleration of a turboshaft engine during a restart”, *ASME GT2018-76654*, 2018
- [4] S. R. GAUDET, J. E. D. GAUTHIER, “A simple sub-idle component map extrapolation method”, *ASME GT2007-27193*, 2007

-
- [5] J. HÖNLE, M. KERLER, H. NACHTIGALL, W ERHARD, H.-P. KAU, “Experimental validation of a sub-idle compressor map extrapolation”, *ISABE-2013-1125*, 2013
- [6] ZHITAO WANG, YI-GUANG LI, HUI MENG, SHUYING LI, NINGBO ZHAO, “Method of extrapolating low speed compressor curves based on improved similarity laws”, *ASME GT2015-44108*, 2015
- [7] J. KURZKE, “Compressor and turbine maps for gas turbine performance computer programs”, Issue 3, 2012. Available from GasTurb GmbH, Aachen, Germany (www.gasturb.de)
- [8] D. LIPPETT, G. WOOLLATT, P.C. IVEY, P. TIMMIS, B.A. CHARNLEY, “The design, development and evaluation of 3D aerofoils for high speed axial compressors. Part 1: Test facility, instrumentation and probe traverse mechanism”, *ASME GT2005-68792*, 2005
- [9] P. K. ZACHOS, I.ASLANIDOU, V. PACHIDIS, R. SINGH “A sub-idle compressor characteristic generation method with enhanced physical background”, *Journal of Engineering for Gas Turbines and Power*, Vol 133, August 2011
- [10] N. CUMPSTY, A. HEYES, “Jet Propulsion”, *Cambridge University Press*, Third Edition, page 149, 2015
- [11] I. ASLANIDOU, P.K. ZACHOS, V. PACHIDIS, R. SINGH “A physically enhanced method for sub-idle compressor map generation and representation”, *ASME GT2010-23562*, 2010
- [12] P. K. ZACHOS, “Gas turbine sub-idle performance modelling; altitude relight and windmilling”, Ph. D. Thesis, *Cranfield University, School of Engineering Department Of Power And Propulsion* 2010
- [13] J. KURZKE “How to get component maps for aircraft gas turbine performance calculations”, *ASME Paper 96-GT-164*, 1996
- [14] J. KURZKE “An enhanced off-design performance model for single stage fans”, *ASME Paper GT2014-26449*, 2014
- [15] JOACHIM KURZKE, IAN HALLIWELL “Propulsion and Power – An Exploration of Gas Turbine Performance Modeling”, Springer International Publishing AG, ISBN 978-3-319-75977-7, 2018